



NUMERICAL MODELING OF REINFORCED SOIL RETAINING WALLS SUBJECTED TO BASE ACCELERATION

Magdy M. EL-EMAM¹, Richard J. BATHURST² and Kianoosh HATAMI³

SUMMARY

A series of reduced-scale shaking table tests and numerical simulation studies were carried out at the Royal Military College (RMC) of Canada to investigate the response of reinforced soil retaining walls to base acceleration. The wall models were 1 m high by 1.4 m wide by 2.4 m long and were constructed with a uniform sand backfill. The physical test results were used to verify a numerical model that was developed using the program FLAC. The soil material properties were determined by selecting parameters that resulted in a good match between physical direct shear box tests and simulated test results using FLAC. The paper presents comparisons between the numerical results and the response of the reduced-scale model tests to a stepped-amplitude base acceleration function. The largely satisfactory agreement between the measured and predicted wall response results provides confidence in the choice of material models adopted and their implementation within a FLAC code. Implications of the results to current pseudo-static seismic design methods for reinforced soil walls are discussed.

INTRODUCTION

Numerical modeling techniques are powerful tools that have been used to study the static and dynamic behavior of reinforced soil structures (e.g., Richardson [1], Segrestin and Bastick [2], Bathurst and Hatami [3]). Cai and Bathurst [4] carried out dynamic finite element modeling of geosynthetic reinforced segmental (modular block) retaining walls to investigate load-deformation response under simulated earthquake load. Their results showed that these structures performed well for the range of peak acceleration and duration of excitation investigated, despite the relatively poor facing-block interface shear characteristics. In addition, maximum incremental dynamic reinforcement loads were shown to occur at the top of the wall. Bathurst and Hatami [3] used a FLAC code (Itasca [5]) to investigate the influence of different model design parameters on dynamic response of a geosynthetic reinforced soil

¹ Assistant Professor, Structural Engineering Department, Faculty of Engineering, Zagazig University, Egypt. Email: elemam_m@hotmail.com

² Professor and Research Director, GeoEngineering Centre at Queen's-RMC, Royal Military College of Canada, Kingston, Ontario. Email: bathurst-r@rmc.ca

³ Associate Research Director, GeoEngineering Centre at Queen's-RMC, Department of Civil Engineering, Royal Military College of Canada, Kingston, Ontario. Email: hatami-k@rmc.ca

retaining wall with a full-height rigid panel facing. They determined that the reinforcement loads were typically greatest at the connections with the panel facing. However, a major factor influencing wall lateral displacement and reinforcement loads was the type of boundary condition at the toe of the rigid wall face.

In this paper, the results of reduced-scale shaking table tests have been used to verify a FLAC numerical model for dynamic analysis of reinforced soil walls. First, brief descriptions of the physical tests and numerical models are presented. Next, a numerical model is described, that was used to simulate direct shear tests on backfill soil samples. Finally, the numerical results are compared with the measured response of reduced-scale wall models tested on the shaking table and predicted performance using current pseudo-static seismic design methods (i.e. AASHTO [6], Bathurst (NCMA) [7]).

SHAKING TABLE TESTS

Figure 1 shows an example reinforced soil wall model with a full-height rigid facing. A schematic cross section of a typical 1/6-scale model wall and instrumentation layout is shown in Figure 2. The soil reinforcement was a polyester (PET) geogrid material placed in four or five layers and with a reinforcement length to height ratio $L/H=0.6$ or $L/H = 1$. The model walls were designed in accordance with similitude rules proposed by Iai [8], to ensure that the geometry of the walls and stiffness of the geosynthetic reinforcement were representative of the same structures at field-scale. In order to isolate the influence of the toe boundary condition on the model response, two different toe arrangements were used. In the first arrangement (hinged toe), the wall toe was restrained from relative movement (i.e. relative to the shaking table) in the vertical and horizontal directions, while it was free to rotate. In the second arrangement (sliding toe), the toe was free to slide horizontally and rotate, but it was restrained from vertical movement. Additional details of the model configurations and a description of the RMC shaking table facility are reported by El-Emam et al. [9].

The backfill for the reduced-scale test walls was a uniformly graded sand, with angular to sub-angular particles. The relative density of the sand after being compacted using horizontal vibration of the shaking table was practically the same in all tests. The shear strength properties of the sand backfill are shown in Table 1a. The reinforcement was a knitted polyester (PET) geogrid with the material properties given in Table 1b.

The horizontal base acceleration was a stepped-amplitude sinusoidal function with a predominant frequency of 5 Hz (Figure 3), which was significantly smaller than the estimated fundamental frequency of the test walls (22 Hz). One-second time windows illustrating the sinusoidal shape of the input motion are shown in Figure 3b. The frequency content of the input base acceleration is shown in Figure 3c. The acceleration amplitude of the table in each test was increased from the at-rest condition in 0.05g increments held for 5 seconds until excessive model deformation occurred.

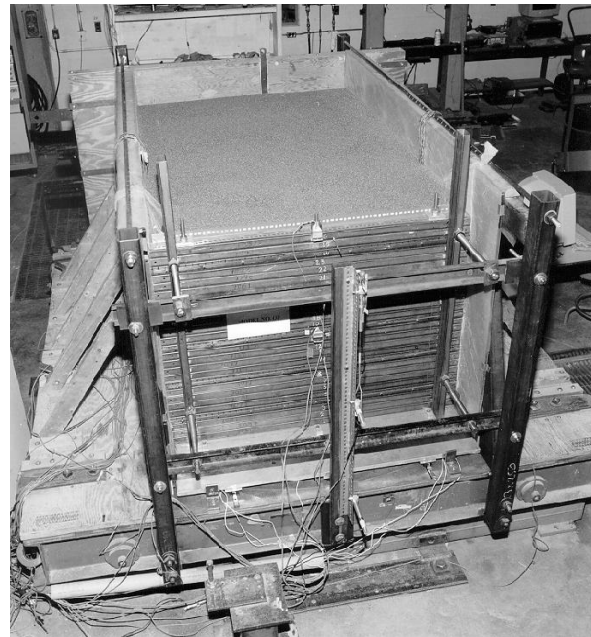


Figure 1. 1/6-scale reinforced soil model wall with vertical full-height rigid facing panel.

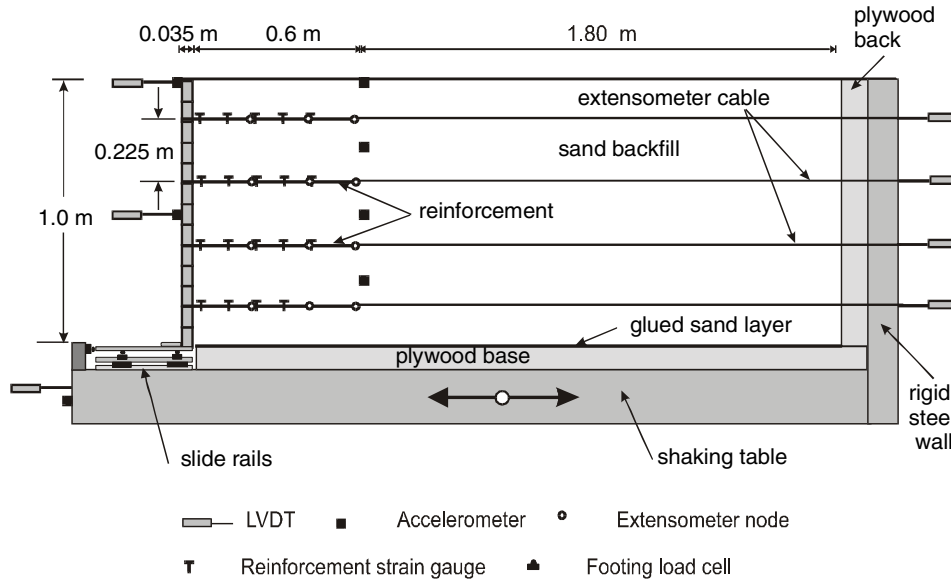


Figure 2. Cross-section of typical 1/6-scale shaking table model wall and instrumentation.

DYNAMIC MODELING OF REINFORCED SOIL WALLS USING FLAC

Figure 4 shows a typical plane-strain numerical model of a reduced-scale reinforced-soil wall with vertical facing panel configuration.

Backfill

The backfill was modeled as a cohesionless material with elastic plastic response and Mohr-Coulomb (M-C) failure criterion. The plastic response of the soil was simulated with a strain softening model and a dilation angle. The values of peak friction angle, ϕ_{peak} , residual friction angle, ϕ_{res} , and dilation angle, ψ

Table 1. Backfill soil and reinforcement material properties.

a) Backfill soil

Properties	Values
Unit weight, γ	15.7 kN/m ³
<u>From direct shear tests</u>	
Peak friction angle, ϕ_{peak}	51°
Residual friction angle, ϕ_{res}	46°
Dilation angle, ψ	15°
Cohesion	0
<u>From FLAC plane-strain model</u>	
Peak plane-strain friction angle, ϕ_{ps}	58°
Residual friction angle, ϕ_{res}	46°
Dilation angle, ψ	15°
Shear Modulus, G	7 MPa
Bulk Modulus, K	6 MPa

b) Reinforcement material

Properties	Values
Compressive strength, T_{comp}	0
Thickness, t	0.002 m
<u>From wide-width tensile tests</u>	
Axial stiffness, $J_{(2\%)}^*$	90 kN/m
Yield strength, T_{yield}	13 kN/m
<u>Used in FLAC model</u>	
Elastic modulus, $E_{(2\%)} = J_{(2\%)} / t$	45 MPa
Yield strength, T_{yield}	6.5 MPa
Cross section area, A	0.002 m ²
Perimeter, P	2 m

* taken at 2% axial strain

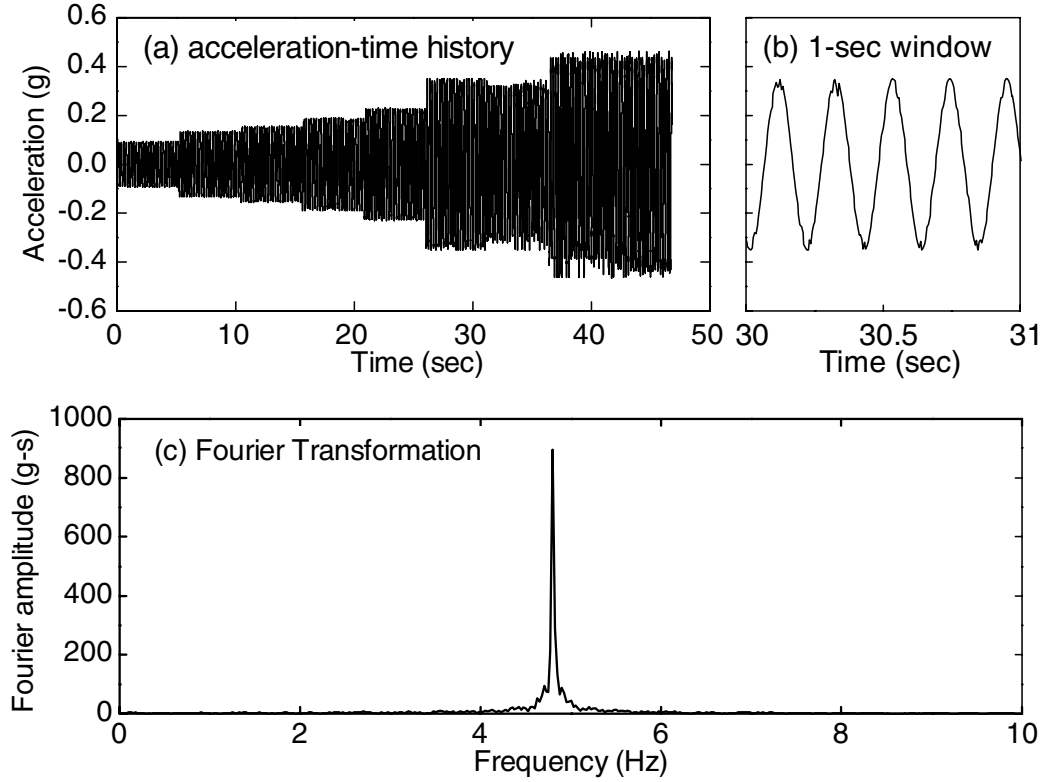


Figure 3. Input base acceleration used in reduced-scale shaking table models and FLAC numerical models.

were measured in the laboratory using conventional direct shear tests and by back-fitting soil parameter values to achieve a match between the FLAC direct shear test model (Figure 5) and measured boundary loads and displacements. The numerical calibration exercise was carried out by adjusting the soil shear modulus, G , bulk modulus, K and peak plane-strain friction angle, ϕ_{ps} until the predicted variations of stress ratio τ/σ_n and vertical displacement with horizontal shear displacement gave a satisfactory match with measured data (Figure 6). During this calibration procedure, the soil unit weight, γ , dilation angle, ψ , and residual friction angle, ϕ_{res} were kept constant. The measured backfill soil properties and the corresponding values from the FLAC plane-strain model are summarized in Table 1a.

Reinforcement

The reinforcement was modeled using linear-elastic perfectly plastic cable elements with no compressive strength. The cable elements were rigidly attached to the numerical grid points of the backfill and the facing panel. Therefore, no relative movement between the backfill grid points and reinforcement nodes was allowed. The cable element properties used in FLAC are elastic modulus, E , tensile yield strength, T_{yield} and compressive yield strength, T_{comp} . The stiffness of the geogrid reinforcement ($J = E \times t$) was determined from in-isolation, rapid loading rate (i.e. 20% strain/min) tensile tests. Wide-width test results carried out in this investigation and previous work by Bathurst and Cai [10] have demonstrated that the modulus of PET geogrid materials is, for practical purposes, independent of rate of loading. A review of in-soil testing reported by Walters et al. [11] shows that the tensile modulus of the knitted PET geogrid used in this study is not modified by soil confinement for typical depths of burial in the field. Table 1b shows the properties of the reinforcement material from laboratory measurements and values used in the FLAC numerical model.

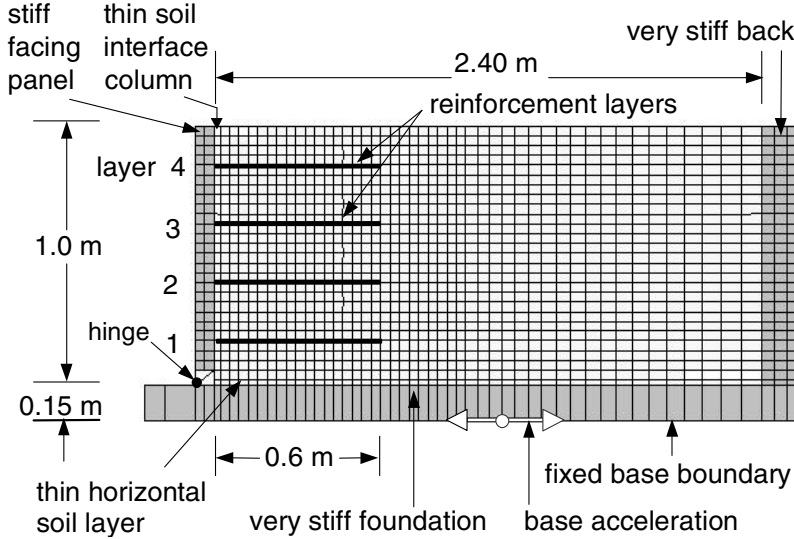


Figure 4. Example numerical grid for the reinforced soil model walls with hinged toe and vertical facing.

Facing panel

Four-noded, linear elastic continuum zones were used to model the full-height facing panel, as shown in Figure 4. The facing panel unit weight, shear modulus and bulk modulus values were taken as $\gamma = 17.2 \text{ kN/m}^3$, $G_w = 1000 \text{ MPa}$, and $K_w = 1100 \text{ MPa}$, respectively. The foundation (i.e. shaking table) and the far-end boundary regions shown in Figure 4 were assigned the same material properties as those used for the facing panel.

Interfaces

The interface between the backfill soil and the foundation was modeled using a thin (0.02 m-thick) soil layer placed directly on the foundation (Figure 4). The material properties of this layer were the same as those of the backfill material. This approach is consistent with the arrangement in the shaking table model tests where a layer of backfill sand was glued to the table surface to create a frictional boundary interface. The interface between the reinforced soil and the facing panel was modeled using a thin (0.015 m-thick) soil column directly behind the facing panel (Figure 4). The soil-facing panel interface material properties were the same as the backfill properties except that the interface friction angle was taken as $\delta = 3/4\phi_{ps}$. This value was initially determined from FLAC parametric analysis to match the measured and predicted horizontal and vertical toe loads at end of construction. Hatami and Bathurst [12] determined the friction angle between the facing column and the backfill from the measured toe reactions and sum of the measured connection loads in full-scale wall tests using the following equation:

$$\delta = \tan^{-1} \left(\frac{R_V - W_f}{R_H + \sum T_i} \right) + \omega \quad (1)$$

where R_V and R_H are the measured vertical and horizontal components of the toe reaction, respectively, W_f is the weight of the facing panel, $\sum T_i$ is the sum of the total connection loads, and ω is the facing panel batter angle from the vertical. Variation of back-calculated friction angle, δ from Equation 1, with input base acceleration amplitude is shown in Figure 7 and shows good agreement with the assumed value in numerical models.

Temporary supports and wall construction

During the construction of shaking table model walls, the full-height facing panel was fully supported in the horizontal direction. In the numerical models, the temporary supports were modeled by fixing the front nodes of the facing panel in the horizontal direction during construction. Each model wall was constructed in twenty-six layers, and was solved to static equilibrium after the placement of each soil layer. After removing the facing temporary supports, the model wall was solved to static equilibrium to determine the wall end-of-construction response before the application of the input base motion.

Damping

A constant damping ratio of $\xi = 5\%$ was assigned to the backfill and facing element zones. It has been shown that the damping ratio of sand is strongly dependent on cyclic shear strain amplitude (e.g. Kramer [13], Ishihara [14]). However, a parametric study by Bathurst and Hatami [3] showed that a reduction in backfill damping ratio from 10% to 5% in a 6 m-high model wall led to only about an 8% increase in the maximum reinforcement load and a 15% increase in lateral displacements. The reason is that the

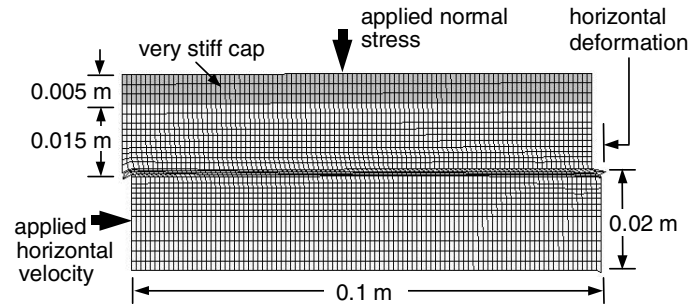


Figure 5. Deformed two-dimensional numerical model of direct shear test simulation for backfill sand.

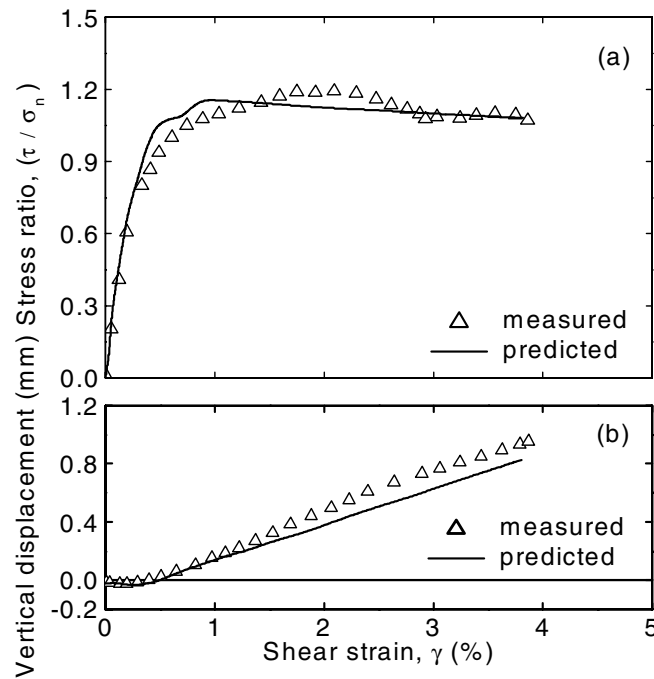


Figure 6. Measured and simulated direct shear test results for backfill sand: (a) stress ratio, (b) vertical displacement.

dissipation of input energy in the model reinforced soil walls occurs largely through the plastic deformation of the soil in the failure zone (i.e. near-field) directly behind the facing. This same zone is largely responsible for the magnitude of facing displacement and reinforcement load predicted during base excitation. Therefore, the magnitude of damping ratio assigned to the backfill soil beyond the reinforced zone (i.e. far field) will not have a significant influence on the predicted response of the test walls.

Input motion

A stepped-amplitude sinusoidal velocity function with a frequency of 5 Hz and zero vertical velocity was applied horizontally to all nodes on the boundary at the foundation level (Figure 4). The input velocity amplitude was increased every 5 seconds in 0.05g base acceleration increments (Figure 3a) until excessive model deformation occurred. The velocity time histories were calculated such that their numerical differentiation would give input base acceleration amplitudes matching those used in the physical shaking table tests.

COMPARISON OF PREDICTED AND MEASURED WALL RESPONSE RESULTS

Facing horizontal displacement at top of wall

Predicted and measured time histories of the peak lateral displacement at the top of the wall-facing panel for hinged and sliding toe model walls are shown in Figures 8a and 8b, respectively. The predicted and measured time histories of the peak lateral displacement at the base of the sliding toe wall are also shown in Figure 8b. The predicted facing lateral displacement for the hinged toe model from numerical simulation results is in satisfactory agreement with the experimental data. The predicted top lateral displacement of the sliding toe model wall showed better agreement with the measured data than the lateral displacement at the bottom (i.e. toe). The measured maximum toe displacement was over-predicted by about 30%. A possible reason for this overestimation may be the difference between the in-isolation and in-soil axial stiffness values of the reinforcement geogrid under very low confining pressures. In the physical model tests, the bottom layers are better confined, and therefore their in-soil axial stiffness may be greater than the measured in-isolation stiffness. However, in the numerical models the same constant in-isolation axial stiffness value was used for all reinforcement layers. Alternatively, the discrepancy could be due to the use of a perfect bond at the reinforcement-soil interface as discussed later in the paper. A perfect interface bond model precludes possible slip between the reinforcement and sand backfill in numerical simulations.

The results shown in Figure 8 indicate that both hinged and sliding toe model walls experienced excessive lateral deformation (i.e. became unstable) at about 35 to 37 seconds from the start of the tests when the input base acceleration amplitude became greater than 0.3g. This acceleration amplitude is considered the critical acceleration value for the two model walls. Typical deformation shapes at the end of base acceleration for both numerical and physical walls are shown in Figure 9. Both numerical and shaking table tests revealed a

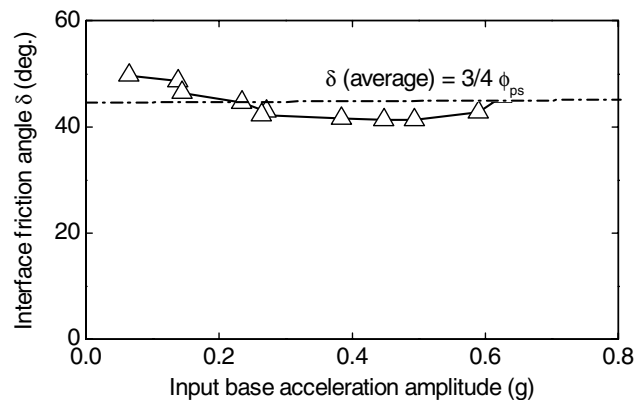


Figure 7. Variation of facing-backfill soil friction angle (calculated from measured toe reactions) with input base acceleration amplitude.

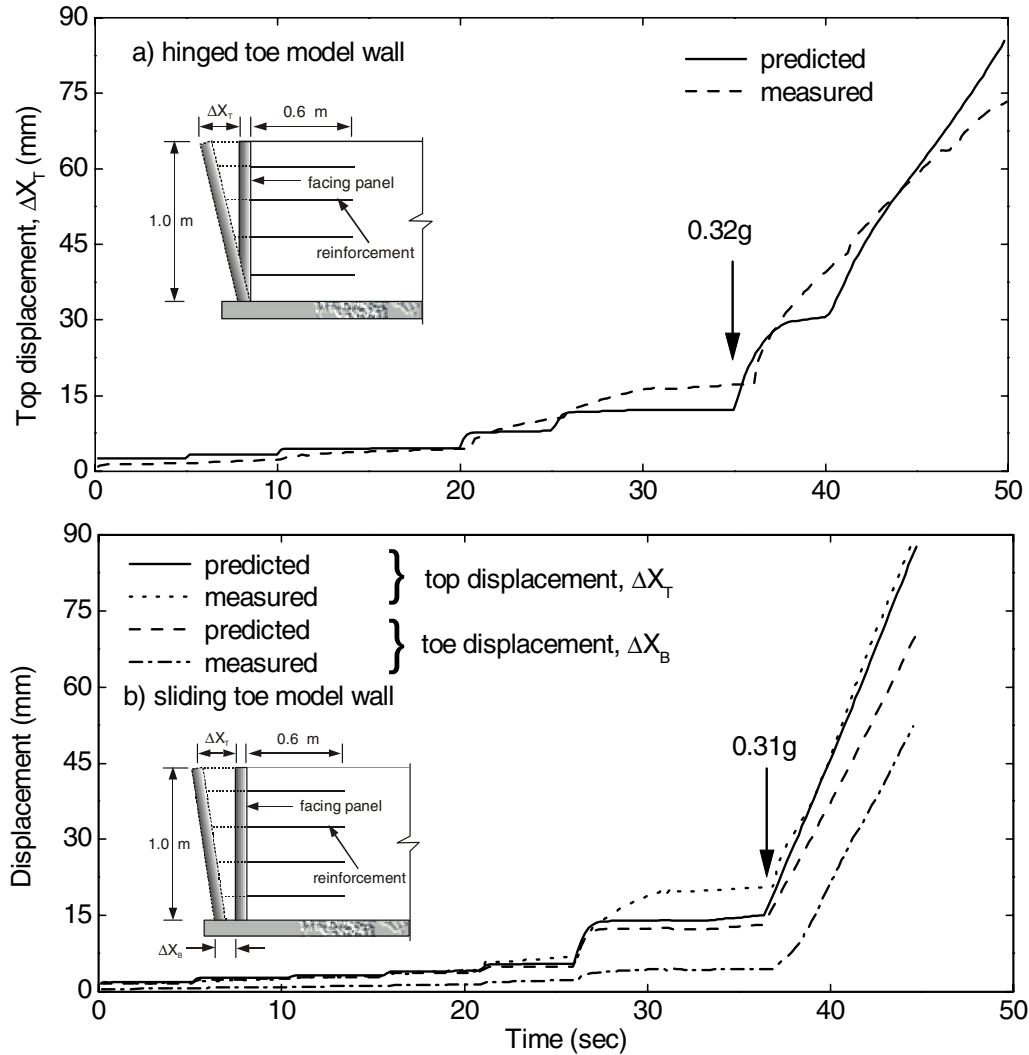


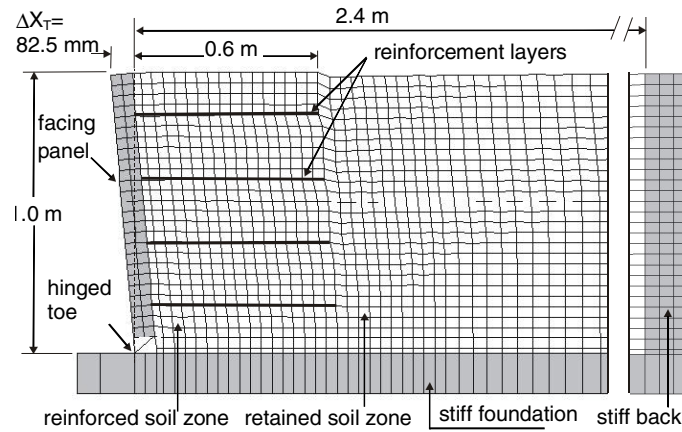
Figure 8. Predicted and measured time histories of the peak facing lateral displacement at the top and bottom of the facing panel for hinged and sliding toe model walls.

local backfill surface slump at the end of the reinforced soil zone. The reinforced soil zone with the facing panel deformed as a parallel-sided monolithic mass.

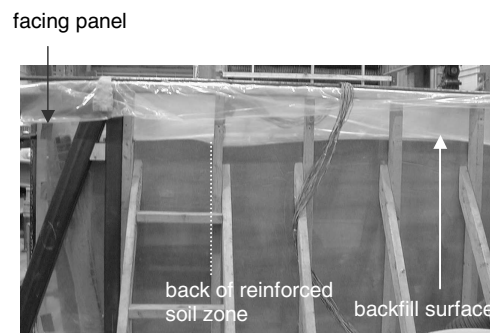
Predicted and observed soil failure mechanisms

Shear zones within the reinforced and retained soil zones of a numerical model wall at two different input base acceleration amplitudes are shown in Figure 10 together with linear failure surfaces predicted from Mononobe-Okabe (M-O) earth pressure theory. Observed internal failure surfaces are indicated with broken lines in Figure 10. The numerical model showed a well-defined failure surface that intersected all reinforcement layers at low input base acceleration amplitudes (Figure 10a) but extended beyond the upper reinforcement layers at greater input base acceleration amplitudes (Figure 10b). The failure zone geometry can be approximated by a single wedge at low input base acceleration amplitudes (i.e. $\alpha_g \leq 0.3g$) and by a two-part wedge at higher base acceleration amplitudes (i.e. $\alpha_g > 0.3g$). The break point for the two-part wedge mechanism is located at the back of the reinforced zone. The failure surfaces from shaking table tests are in reasonable agreement with the shear zone geometry from the numerical model at high input base acceleration amplitudes (Figure 10b). At lower input base acceleration amplitudes (Figure 10a),

the shear zone boundaries from the numerical model are in good agreement with the failure surface calculated using the (M-O) pseudo-static method. Hence, pseudo-static equilibrium methods may be useful to determine the shear zone boundaries at relatively low acceleration amplitudes (i.e. $\alpha_g < 0.27g$). However, for greater input base acceleration amplitudes, pseudo-static equilibrium methods tend to underestimate the volume of the shear zone. Figure 10b illustrates that the bottom reinforcement layers are extremely important in resisting seismic forces at higher input base acceleration amplitudes. As the failure surface propagated towards the back of the model wall, the top reinforcement layers were contained within the failure wedge. Therefore, seismic loads were transferred to the bottom reinforcement layers which still had significant anchorage capacity within the reinforced soil zone.



a) numerical model deformation



b) reduced-scale shaking table model

Figure 9. Predicted and observed deformed shape of the hinged model wall (4 reinforcement layers and $L/H = 0.6$) at the end of base excitation.

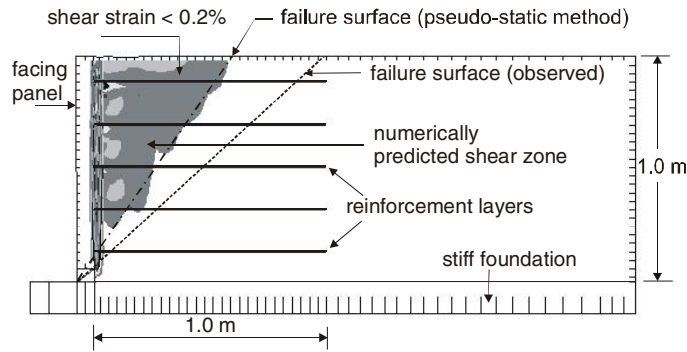
Reinforcement loads

Reinforcement load-time histories

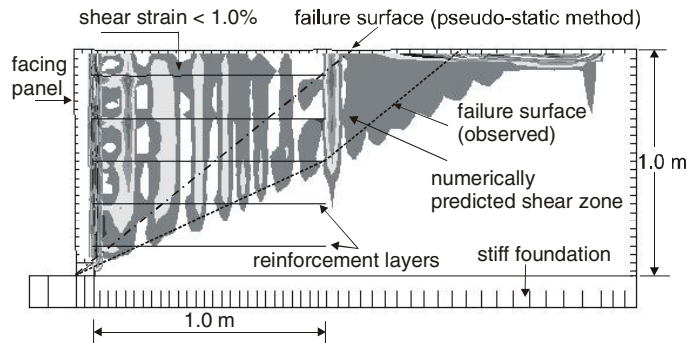
Example predicted and measured time histories of the peak axial reinforcement load at the back of the facing panel (i.e. connection loads) for the hinged toe model wall are shown in Figure 11. Both the measured and predicted connection loads can be seen to accumulate with time during base excitation. With the exception of the top reinforcement layer, the numerical model gave satisfactory prediction of the reinforcement connection loads for the first 35 seconds of the test, when $\alpha_g < 0.3g$. The numerical model over-predicted the reinforcement connection loads for base acceleration amplitudes greater than $0.3g$. Moreover, the numerical model predicted greater connection load magnitudes in the top reinforcement layer at all stages in the simulation run. This is due to the perfect bond that was assumed at the interfaces between the reinforcement elements and soil zones in the numerical model. This perfect bond allows large load magnitudes to be mobilized in the reinforcement layer in the wall numerical model. In contrast, the top reinforcement layer in the physical model is not perfectly bonded to the surrounding soil due to low overburden pressure. Therefore, upper reinforcement layers in the physical walls have likely slipped inside the backfill during base excitation. Figure 11 shows that the connection loads in the bottom layer were predicted with better accuracy. The reason is that the bottom layer was better confined and potential slippage at the reinforcement-sand interface was reduced.

Reinforcement load distributions

Figure 12 shows the predicted and measured reinforcement loads deduced from strain gauge readings for both hinged and sliding toe model walls at end of construction and at $\alpha_g = 0.4g$. The magnitude and distribution of reinforcement loads from the numerical models are in reasonable agreement with the



a) acceleration amplitude = 0.15g



b) acceleration amplitude = 0.5g

Figure 10. Predicted and observed failure surfaces from hinged toe model wall (5 reinforcement layers and $L/H = 1.0$) at different input base acceleration amplitudes. Note: Dark shading indicates large shear strains.

measured data. Results shown in Figure 12 indicate that the numerical model over-predicts the connection loads in the upper reinforcement layer during base excitation. The reasons for this over-prediction have been discussed in the previous section. Nevertheless, the results shown in Figure 12 indicate that the numerical model was able to capture the effect of the toe boundary condition on the distribution of reinforcement loads (e.g. reinforcement loads were very much higher in the bottom reinforcement layer for the sliding toe model than for the hinged toe model).

Reinforcement connection loads

The distribution and magnitudes of the measured and predicted reinforcement connection loads in model walls with hinged and sliding toe conditions at end of construction (i.e. static loading) and at different input base acceleration amplitudes (i.e. dynamic loading) are plotted in Figure 13. The connection loads calculated using the two main seismic design methods for geosynthetic reinforced soil walls (i.e. Bathurst (NCMA) [7] and AASHTO [6]) are also shown in the figure. The accuracy of predicted connection loads over the middle height and at the toe of the wall models is reasonably good for base acceleration amplitudes up to 0.3g. However, the numerical models predict greater load magnitudes in the top reinforcement layers in both hinged and sliding toe model walls. This is likely due to reinforcement-soil slippage, which was not modeled in numerical simulations. This observation highlights the requirement to include slip interfaces in numerical models for reinforcement layers under low overburden pressures.

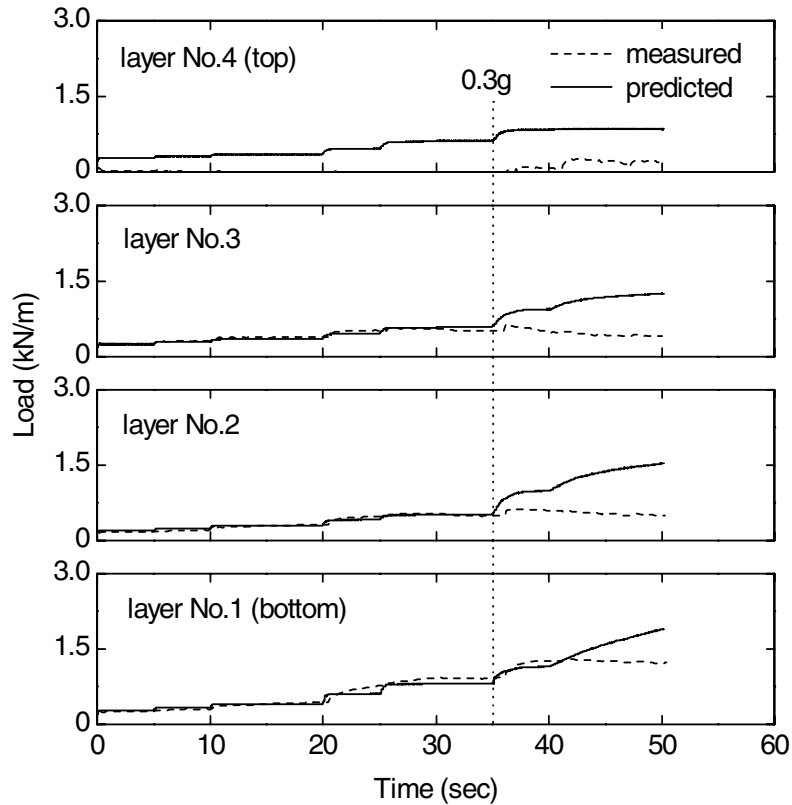


Figure 11. Predicted (numerical) and measured peak connection load-time histories for reinforcement layers in typical hinged toe model wall (4 reinforcement layers and $L/H = 0.6$).

The numerical results in Figure 13 demonstrate that the facing toe attracted a significant portion of the total horizontal earth pressure at all stages of the simulation for the hinged toe model and therefore reduced the load demand on the reinforcement layers. For the sliding toe model wall, both numerical and experimental models predicted significant connection loads at the bottommost reinforcement layer of the wall to compensate for the lack of toe support.

The predicted distributions of connection loads from current seismic design methods in Figure 13 contain the numerical and measured values for the hinged toe model wall and capture the trends in values for acceleration amplitudes up to 0.3g. The reinforcement load distribution calculated using the NCMA design method is in good agreement with the distribution predicted from the numerical model at 0.4g. Nevertheless, neither design method considers the toe restraint effect when calculating the magnitude and distribution of reinforcement connection loads.

The numerical and measured connection loads in the example sliding toe model wall are in reasonably good agreement for input base acceleration amplitudes up to 0.2g (Figure 13). However the numerical and analytical methods underestimate the measured connection load in the bottommost layer. Both analytical and numerical methods over-predicted the connection loads at the topmost layer at acceleration amplitudes greater than 0.2g.

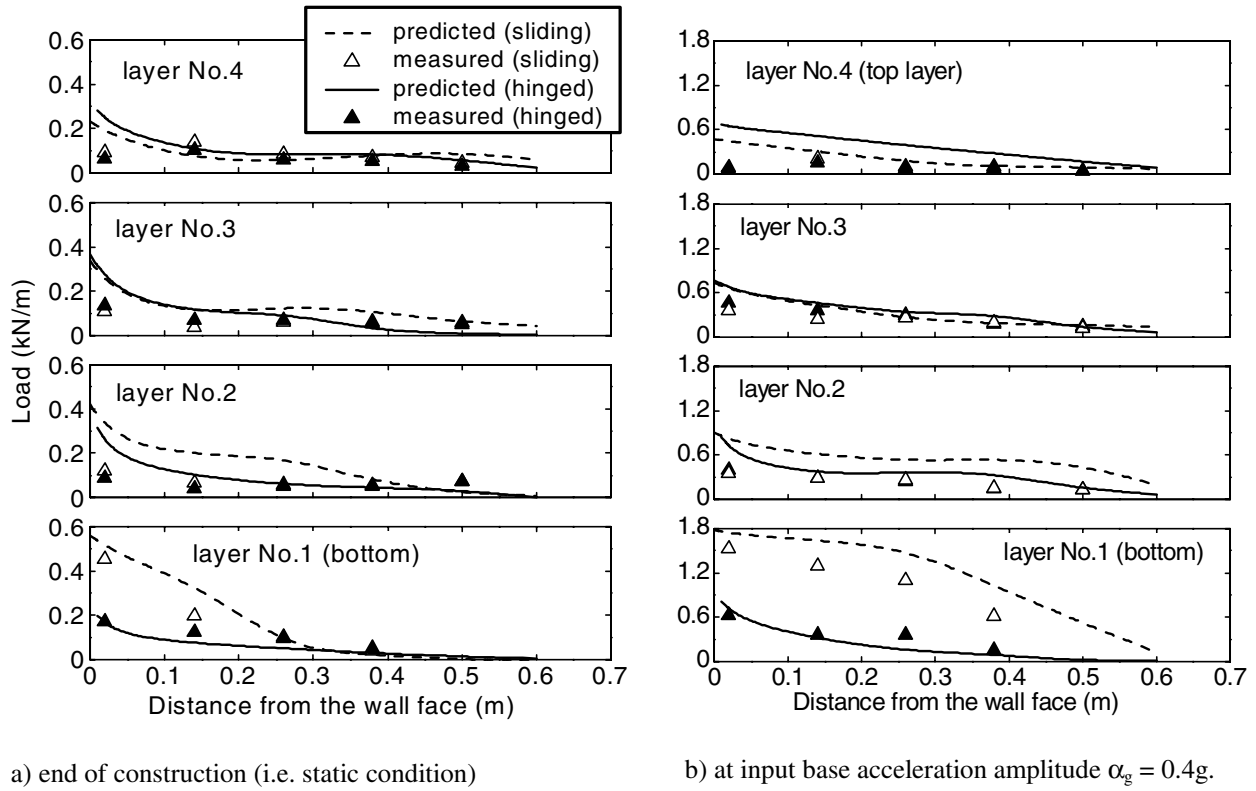


Figure 12. Predicted (numerical) and measured reinforcement load distributions for typical hinged toe model wall.

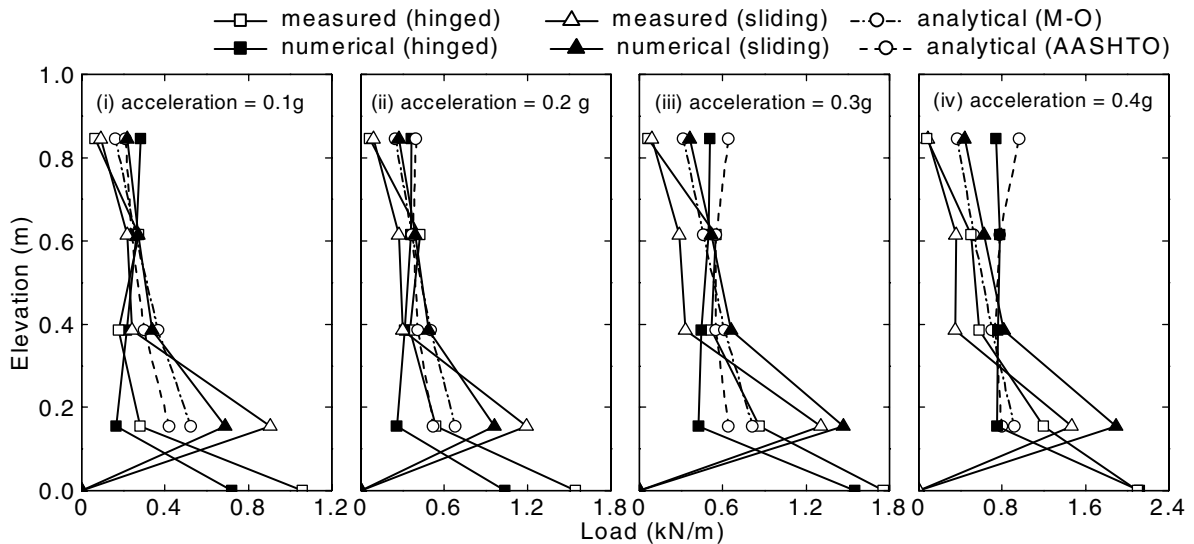


Figure 13. Connection loads and horizontal toe loads at different input base acceleration amplitudes for hinged toe model wall from experimental, numerical and analytical models.

Toe loads

Figure 14 shows time histories of the measured and predicted vertical and horizontal toe loads for a hinged toe model wall during base excitation. The figure also includes the vertical toe load history of the sliding toe model wall. The predicted vertical and horizontal toe loads show satisfactory agreement with

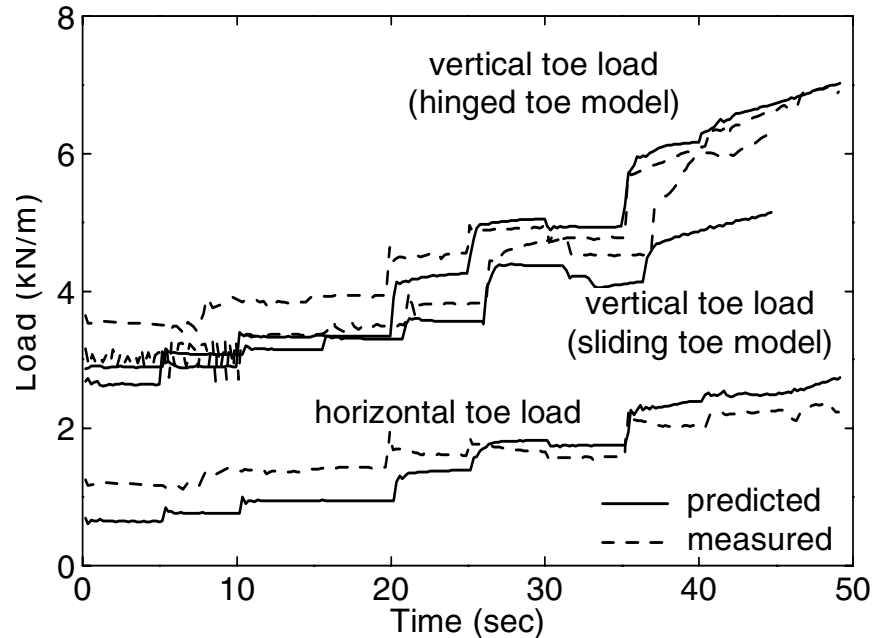


Figure 14. Predicted (numerical) and measured time histories of the peak vertical and horizontal toe loads for hinged and sliding toe model walls.

the measured values for both model walls at end of construction (i.e. $t = 0$) and during base excitation. Both numerical and experimental results indicate a slightly greater vertical toe load magnitude for the hinged toe model wall compared to the sliding toe model wall which can be attributed to the larger soil mass that moved outward beyond the wall toe as a result of greater outward rotation of the facing panel. Figure 14 also shows that the numerical model slightly under-predicted both vertical and horizontal toe reaction components for $\alpha_g < 0.2g$. However, the difference between measured and predicted values is considered to be within the accuracy of the instrumentation and test repeatability.

Earth pressure resultant

Figure 15 shows a comparison between the measured and predicted total earth force acting on the facing panel during base excitation. The total earth force is equal to the summation of all reinforcement connection loads (i.e. $\sum T_i$) in the sliding toe model wall, and the summation of reinforcement connection loads plus the facing toe horizontal reaction (i.e. $\sum T_i + R_H$) in the hinged toe model wall. The numerically predicted horizontal earth force is in close agreement with the measured data for the hinged toe model wall. However, the predicted earth force values for the sliding toe model subjected to strong base acceleration (e.g., $\alpha_g > 0.2g$) are greater than measured values. The difference for the sliding model case is attributed to the slippage of reinforcement within the backfill soil, which results in lower reinforcement connection loads compared to the case when the slippage of reinforcement is prevented. The results shown in Figure 15 indicate that both pseudo-static seismic design methodologies underestimated the measured and predicted values of the total earth force behind the hinged toe model wall. However, for the sliding toe model wall, the calculated values from current design methods give values that fall between measured and numerical results.

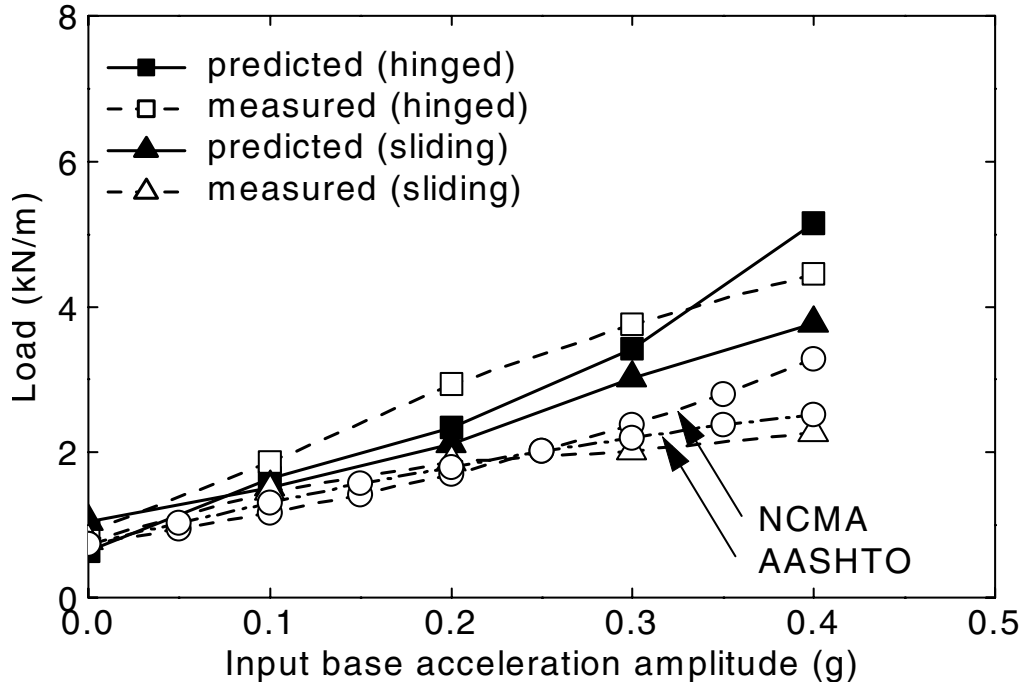


Figure 15. Measured and predicted earth pressure resultant at the back of the facing panel vs. input acceleration amplitude for hinged and sliding toe model walls.

CONCLUSIONS

In this paper, experimental and numerical results of selected reinforced model walls with a full-height propped panel facing that were tested on the RMC shaking table are presented. The numerical simulations were carried out using the commercially available finite difference based program FLAC. Some additional comparisons with analytical predictions using current pseudo-static design methods are also shown. Based on the results of this research program the following conclusions can be made:

1. Soil plane-strain material properties back-calculated from numerical simulation of physical direct shear tests on backfill samples were required to generate good agreement between physical and numerical wall response features.
2. A constant reinforcement stiffness value was shown to be a reasonable assumption for numerical modeling of the geogrid reinforcement. However, reinforcement-soil slip for layers with shallow overburden depth was not considered in numerical simulations and this is thought to have led to some discrepancies in reinforcement load response close to the top of the wall.
3. Notwithstanding the comments made above, the numerical model was found to give reasonably accurate predicts of the experimental results despite the complexity of the physical models under investigation.
4. Both numerical and physical models demonstrated that the toe boundary condition has a large influence on wall performance and stability under both static and simulated seismic loading conditions.
5. Both numerical and experimental models showed that current pseudo-static seismic design methods may underestimate the size of the soil failure zone behind the wall facing, particularly at large input base acceleration amplitudes and these analytical methods are unable to explicitly account for the influence of the toe boundary reactions on wall response.

REFERENCES

1. Richardson, G.N. "The Seismic Design of Reinforced Earth Walls." Report to the National Science Foundation, UCLA-ENG.-7586, 1976.
2. Segrestin, P. and Bastick, M.J. "Seismic design of reinforced earth retaining walls - the contribution of finite element analysis." Proc. International Symposium on Theory and Practice of Earth Reinforcement, IS-Kyushu '88, Fukuoka, Japan, October 1988: 577-582.
3. Bathurst R.J. and Hatami, K. "Seismic response analysis of a geosynthetic-reinforced soil retaining Wall." Geosynthetics International, 1998; 5 (1-2): 127-166.
4. Cai, Z. and Bathurst, R.J. "Seismic response analysis of geosynthetic reinforced soil segmental retaining walls by finite element method." Computers and Geotechnics 1995; 17(4): 523-546.
5. Itasca Consulting Group. FLAC - Fast Lagrangian Analysis of Continua, v 4.00, Itasca Consulting Group Inc., Minneapolis, MN, USA, 2001.
6. AASHTO. "Standard specifications for highway bridges." 17th edition. American Association of State Highway and Transportation Officials, Washington, DC, USA, 2002.
7. Bathurst, R.J. "NCMA Segmental Retaining Wall Seismic Design Procedure – Supplement to Design Manual for Segmental Retaining Walls (Second Edition 1997)." National Concrete Masonry Association, Herndon, VA, USA, 1998, 187 p.
8. Iai, S. "Similitude for shaking table tests on soil-structure-fluid models in 1-g gravitational field." Soils and Foundations, 1989; 29 (1): 105-118.
9. El-Emam, M.M., Bathurst, R.J. and Hatami, K. "Effect of reinforcement design on seismic response of reinforced soil retaining walls." ICPMG'02, St. John's, NF, 10-12 July 2002; 1011- 1016.
10. Bathurst, R.J. and Cai, Z. "In-isolation cyclic load-extension behavior of two geogrids." Geosynthetics International, 1994; 1(1): 3-17.
11. Walters, D.L., Allen, T.M., and Bathurst, R.J. "Conversion of Geosynthetic Strain to Load using Reinforcement Stiffness." Geosynthetics International, 2002; 9(5-6): 483-523.
12. Hatami, K. and Bathurst, R.J. Modeling static response of a segmental geosynthetic reinforced soil retaining wall using FLAC. Proc. 2nd International FLAC Symposium. Numerical Modeling in Geomechanics, Lyon, October 2001, 223-231.
13. Kramer, S.L. "Geotechnical Earthquake Engineering." Prentice-Hall, Upper Saddle River, New Jersey, USA, 1996.
14. Ishihara, K. "Soil behavior in earthquake engineering." Clarendon Press, Oxford University, New York, USA, 1996.